

Highly durable inverted-type organic solar cell using amorphous titanium oxide as electron collection electrode inserted between ITO and organic layer

メタデータ	言語: eng 出版者: 公開日: 2017-10-03 キーワード (Ja): キーワード (En): 作成者: メールアドレス: 所属:
URL	https://doi.org/10.24517/00010313

This work is licensed under a Creative Commons Attribution-NonCommercial-ShareAlike 3.0 International License.



Highly durable inverted type organic solar cell using amorphous titanium oxide
as electron collection electrode inserted between ITO and organic layer

Takayuki Kuwabara*¹, Taketoshi Nakayama,² Konosuke Uozumi², Takahiro Yamaguchi¹,
Kohshin Takahashi*¹

1. Graduate School of Natural Science and Technology, Kanazawa University,
Kakuma-machi, Kanazawa, Ishikawa 920-1192, Japan

2. Research Material-Design Laboratory, Komatsu Seiren Co., LTD, 2-5-2 Asahidai, Nomi,
Ishikawa 923-1211, Japan

* Corresponding author: TEL: +81-76-234-4770
FAX: +81-76-234-4800
E-mail: tkuwa@t.kanazawa-u.ac.jp

Submitted to *Solar Energy Materials & Solar Cells*

Abstract

An indium tin oxide/titanium oxide/[6,6]-phenyl C₆₁ butyric acid methyl ester: regioregular poly(3-hexylthiophene)/poly(3,4-ethylenedioxylenethiophene): poly(4-styrene sulfonic acid)/Au type organic solar cell (ITO/TiO_x/PCBM:P3HT/PEDOT:PSS/Au) with 1 cm² active area, which is called “inverted type solar cell”, was developed using an ITO/amorphous titanium oxide (TiO_x) electrode prepared by a sol-gel technique instead of the low functional electrode such as Al. The power conversion efficiency (η) of 2.47 % was obtained by irradiating AM 1.5G-100 mW cm⁻² simulated sunlight. We found that a photoconduction of TiO_x by irradiating UV light containing slightly into the simulated sunlight was required to drive this solar cell. The device durability in an ambient atmosphere was maintained for more than 20 h under continuous light irradiation. Further, when the air-stable device was covered by a glass plate with water getter sheet which was coated by an epoxy UV resin as sealing material, the durability was still higher and over 96 % of relative efficiency was observed even after continuous light irradiation for 120 h.

Key words: organic thin film solar cells, amorphous titanium oxide, air-stable

Main Text

1. Introduction

Much recent attention has been paid to organic solar cells as clean and safe energy source instead of the fossil fuel due to providing lower cost and environment-friendly energy conversion system [1-6]. Organic thin film solar cells with power conversion efficiency (η) of 5 - 6 % have been recently developed by several research groups [7-9], and these results which showed a possibility toward the practical use of organic solar cells are encouraging other researchers in this field.

A few instances have been reported on the stability of the solar cells compared to on the improvement of the conversion efficiency [10-12], although it is very important to increase the stability as well as the conversion efficiency. It is well known that the photodegradation of polymers and polymer/oxide composites, and the degradation at the ITO and the metal electrodes in organic thin film solar cells are caused by reactions with oxygen and water [13]. An Al metal has been often used as the back electrode of the organic solar cells as shown in Figure 1a, which are termed “normal type solar cells”, due to its low work function. The performance for the normal type solar cells with Al electrode degrades in an ambient atmosphere, perhaps because the Al was oxidized to insulator Al_2O_3 at the Al/organic solid interface and the Al diffused into the active layer acted as a recombination site. Lee et al. have reported air-stable “normal type solar cells” with titanium oxide layer being inserted between P3HT:PCBM active layer and Al electrode, then the lifetime in air of the solar cells increased remarkably compared with that of the solar cells without the titanium oxide layer [14]. Therefore, the development of the solar cells using non-corrosive electrode instead of the Al metal electrode such as so-called “inverted type solar cells” as shown in Figure 1b is expected as a promising approach from viewpoints of the durability improvement. Krebs reported that

ITO/ZnO/ZnO:poly-(3-carboxydithiophene) (P3CT)/PEDOT:PSS/Ag inverted type solar cells without sealing maintained 80 % of the initial performance for continuous illumination for 100 h in an ambient atmosphere [15]. In our previous research, we have developed organic thin film solar cells using a non-corrosive Au metal as the back electrode, and an ITO/In or a transparent conducting oxide (TCO)/TiO₂ as the front electrode [16-19]. We reported that the ITO/In/perylene tetracarboxylic derivative/poly(phenylenevinylene) derivative/PEDOT:PSS/Au two-layer type cell showed the power conversion efficiency of 1.9 % and its performance was about the same after irradiating for 1 h in an ambient atmosphere [20]. Thus, we have reported previously that an organic solar cell using a non-corrosive Au metal as the back electrode showed high durability in an ambient atmosphere. Recently, Brabec et al. presented the reports for the inverted type solar cells using an amorphous titanium oxide and a PCBM:P3HT blend film [21, 22]. But these reports hardly give a full detail of the cell characterization. Herein we present the performance and the durability of ITO/TiO_x/PCBM:P3HT/PEDOT:PSS/Au inverted type bulk-heterojunction organic solar cells.

2. Experiments

2.1. Materials.

Titanium(IV) isopropoxide (Ti[OCH(CH₃)₂]₄, 99.999 %), 2-methoxyethanol (CH₃OCH₂CH₂OH, 99.9 %), ethanolamine (EA; NH₂CH₂CH₂OH, 99.5 %), diethanolamine (DEA; NH(CH₂CH₂OH)₂, 99 %), acetyl acetone (AA; CH₃C(O)CH₂C(O)CH₃, 99 %), regioregular P3HT (M_w ~ 87,000), PEDOT-PSS 1.3 wt% dispersion in water, chlorobenzene (CB), 2,6-dichlorotoluene (DCT), and chloroform (CHL) were purchased from Sigma-Aldrich Chemical Co., Inc. 2-Propanol (dehydrated, 99.5 %) was purchased from Kanto Chemical Co.,

Inc. All the chemicals were used as received. ITO substrates ($10 \Omega/\square$) and Au wires were purchased from Furuuchi Chemical Corporation.

2.2. Preparations of TiO_x precursors.

TiO_x precursor solutions were prepared from titanium (IV) isopropoxide, which was mixed with a stabilizer of 2.45 equivalents for Ti source and heated under an N_2 atmosphere with the method described by Kim et al.[7]. Titanium (IV) isopropoxide (2.4 g, 8.44 mmol) was slowly added to 2-methoxyethanol (12.5 mL) cooled by an ice bath to avoid drastic temperature increase, and then the mixture solution was refluxed for 1 h. Further, the solution was cooled by the ice bath, and EA (1.27 g, 20.7 mmol) or DEA (2.18 g, 20.7 mmol) or AA (2.07 g, 20.7 mmol) as the stabilizer was slowly added to its cooled solution, followed by refluxing for 1 h to obtain the TiO_x precursor solution. EA- TiO_x and AA- TiO_x precursor solutions took on orange and yellow, respectively. However, the DEA- TiO_x solution was colorless. The coloration for the EA- TiO_x and the AA- TiO_x was explained as the d-d absorption originated from a titanium complex ion formed by the reaction of titanium (IV) isopropoxide and stabilizer.

2.3. Fabrications of organic thin film solar cells.

The ITO electrode was first ultrasonicated in 2-propanol, and then cleaned in boiling 2-propanol, and subsequently dried in air. In order to prepare a TiO_x thin film acting as the electron collection layer, the precursor solution was spin-coated on ITO being accompanied by hydrolysis in an ambient atmosphere and by heat treatment at 150°C for 1 h. Thereafter, a CB solution or DCT:CHL (1:1 weight ratio) cosolvent solution containing 25 g L^{-1} of P3HT and 20 g L^{-1} of PCBM was spin-coated onto the ITO/ TiO_x substrate, further a PEDOT:PSS aqueous dispersion solution was spin-coated onto its blend film. Finally, an Au metal as the

back electrode was vacuum-deposited on the PEDOT:PSS solid film. The device was heated at 150 °C for an annealing treatment. The effective area of the solar cell was restricted to 1.0 cm². If necessary, the device was covered by a glass plate with water getter sheet (Komatsu Seiren Co., Ltd.), which was coated by an epoxy UV resin as sealing material, in an N₂ filled glove box, the sealing treatment was finally completed by irradiating UV light to the epoxy resin.

2.4. Measurements.

In order to estimate the thickness of each layer in the device, a scanning electron microscopic (SEM) and an atomic force microscopic (AFM) data were recorded using a Hitachi S-4500 SEM apparatus and an SII SPI3800N AFM apparatus, respectively. The photocurrent-voltage (I-V) curves of the solar cells were measured at 5 V min⁻¹ of scan rate in linear sweep voltammetry (LSV) under a solar simulated light AM 1.5G-100 mW cm⁻² by a Kansai Kagakukikai XES-502S solar simulator being calibrated by a EKO MS-601 pyranometer equipped with a silicon diode. Durability test of the solar cells was carried out by an interval LSV measurement in combination with a rest voltage measurement under continuous irradiation of the AM1.5G-100 mW cm⁻² light. All the electric measurements were implemented in an ambient atmosphere using a Hokuto Denko HZ-5000 electrochemical analyzer. All measurements were carried out in an ambient atmosphere, that is, at room temperature of 15~30 °C and under relative humidity of 40~60 %.

3. Results and Discussion

3.1. Effect of TiO_x layer

A cross-sectional SEM image of the ITO/TiO_x/PCBM:P3HT/PEDOT:PSS/Au inverted type solar cell is shown in Figure 1c. The SEM image showed that the device was consisted of

flatly laminated layers in nanometer-order. The thicknesses of the TiO_x film, the blended film, the PEDOT:PSS film and the Au metal layer were ca. 30, 250, 80, and 200 nm, respectively. These results were consistent with the thicknesses estimated by AFM measurement.

Figure 2 shows the photo and dark I-V curves of the inverted type solar cell with and without TiO_x layer. The performance of the cell without TiO_x layer showed the short-circuit photocurrent (J_{sc}) of 4.21 mA cm⁻², the open-circuit voltage (V_{oc}) of 0.52 V, the fill factor (FF) of 0.38, and the power conversion efficiency (η) of 0.82 %, see curve (b) in Figure 2. Whereas, the performance of the cell with EA-TiO_x layer showed $J_{sc} = 6.70$ mA cm⁻², $V_{oc} = 0.56$ V, FF = 0.55, and $\eta = 2.06$ %, see curve (a) in Figure 2, the η value being 2.5 times higher than that without TiO_x layer. This result suggests an improvement of the rectification of the device, because the TiO_x layer acts as an electron collection layer and a hole blocking layer [8, 23].

Figure 3 shows the photo I-V curves of the solar cells with the various TiO_x thin films, and the cell performance is summarized in Table 1. When an EA-TiO_x layer (curve (a) in Figure 3) and an AA-TiO_x layer (curve (c) in Figure 3) were inserted between the ITO substrate and the PCBM:P3HT organic layer, the η values over 2 % were obtained. However the η of the solar cell with a DEA-TiO_x layer (curve (b) in Figure 3) was about 1 %. A decrease of the J_{sc} , the FF and the parallel resistance (R_p / Ω), and an increase of the series resistance (R_s / Ω) in the DEA-TiO_x layer inserted type cell are ascribed to lower electron mobility in the TiO_x bulk and higher TiO_x/PCBM:P3HT interfacial resistance than other TiO_x layer inserted type cells. The DEA-TiO_x precursor solution was colorless, that is, the d-d absorption expected from titanium-DEA complex ions was not observed. After all, the moisture-unstable titanium (IV) isopropoxide was rapidly polymerized by hydrolysis in an ambient atmosphere, resulting in the large electric resistance of the TiO_x sheet because of the formation of large TiO_x particles. Thus, the complex formation by an appropriate stabilizer

such as EA and AA in the precursor solution plays a key role for preparing smaller resistance in the TiO_x bulk and at the $\text{TiO}_x/\text{PCBM:P3HT}$ interface. In addition, the performance ($\eta = 2.31\%$) of the cell with AA- TiO_x layer increased by 10 % compared to that ($\eta = 2.06\%$) with EA- TiO_x layer. This suggests the possibility that a certain amount of stabilizer remains in amorphous TiO_x film prepared from the sol-gel method containing the organic stabilizer, this residual being one of the cell resistance components. The AA stabilizer can be easily removed rather than the EA stabilizer by heat treatment at $150\text{ }^\circ\text{C}$, because the boiling point (b.p.) of AA at $140\text{ }^\circ\text{C}$ is lower than b.p. of EA at $170\text{ }^\circ\text{C}$.

Inset of Figure 3 shows the plots of the η versus the thickness of TiO_x layer. The maximum η values for the devices with EA-, DEA-, and AA- TiO_x layers were obtained in 10 nm to 30 nm range of the thickness. These results suggest that the thicker TiO_x layer is responsible for an increase of the series resistance because the amorphous TiO_x has low conductivity, and further the thinner TiO_x coating causes less rectification property because the TiO_x layer partially covers on the ITO surface. As a result, the optimum thickness existed for each TiO_x layer.

3.2. Influence of photoconduction of TiO_x layer

When the photo I-V curves of an ITO/AA- $\text{TiO}_x/\text{PCBM:P3HT}$ (CB solvent)/PEDOT:PSS/Au inverted type solar cell with blend film prepared by the CB solvent were measured using a UV light cut filter ($\lambda < 420\text{ nm}$), the photocurrent absolutely was not observed even by light irradiation for 1 h as shown in phase 1 (open circle) of Figure 4. But when the UV light cut filter was taken off, the η value suddenly increased. The maximum performance of $J_{\text{sc}} = 7.05\text{ mA cm}^{-2}$, $V_{\text{oc}} = 0.56\text{ V}$, $\text{FF} = 0.53$, and $\eta = 2.12\%$ was obtained after irradiating for 120 min as shown in phase 2 (filled circle) of Figure 4. Further, the photo I-V curves were repeatedly measured under continuous light irradiation with the UV light cut

filter. By using the filter, the η decreased from 2.12 % to 0.04 % as shown in phase 3. And then by removing the filter, the cell performance almost recovered up to the maximum performance of phase 2, the performance of $J_{sc} = 6.76 \text{ mA cm}^{-2}$, $V_{oc} = 0.57 \text{ V}$, $FF = 0.56$, and $\eta = 2.14 \%$ being obtained, see phase 4. Thus, it turned out that UV light irradiation to the solar cell is important for driving this type solar cell. This character of the cell device is attributed to the TiO_x layer. It is noted that the titanium oxide shows a long-period photoconduction property by UV light irradiation.[24, 25] In our case, electrons produced in the TiO_x bulk by irradiating UV light contained slightly in AM 1.5G simulated sunlight may result in relatively smooth charge transport for the photo-produced electrons by the photovoltaic effect.

3.3. Durability of TiO_x layer inserted type solar cell

The durability test was carried out in an ambient atmosphere. The durability observation was measured just after light irradiation. The comparison of the η against irradiation time in the ambient atmosphere for the inverted type organic solar cell with amorphous AA- TiO_x (open square) and the normal type organic solar cell (open circle) is shown in Figure 5, and the cell performance is summarized in Table 2. For the normal type solar cell, the η decreased down to 50 % of the maximum value after light irradiation for 10 h. This result suggests that the oxidation of the Al electrode and the Al diffusion into the active layer lead to the decrease of the cell performance [13]. In contrast, the η for the solar cell with the TiO_x layer instead of the Al electrode was almost maintained under continuous light irradiation for 20 h, and its high durability in the ambient atmosphere was demonstrated because the Au electrode as the back electrode is non-corrosive in air. On the other hand, when a TCO/anatase TiO_2 substrate was employed as the electron collection electrode, the cell performance decreased down to

63.8 % of the maximum η by irradiating in air for 10 h (the data being not showed), probably because of a photo-catalytic effect by anatase TiO_2 .

3.4. Preparations of elegant PCBM-P3HT blend film and long lifetime organic solar cell

In order to improve the energy conversion efficiency of the solar cells, we have attempted to prepare a PCBM:P3HT blend film with better morphology by both of solvent-choosing and drying treatment. Figure 6 shows the photo I-V curves of the solar cells with PCBM:P3HT blend film prepared by CB solvent and DCT:CHL cosolvent. The performance of the cosolvent cell device showed the J_{sc} of 6.90 mA cm^{-2} , the V_{oc} of 0.58 V, the FF of 0.62, and the η of 2.47 %, and slightly increased compared to that ($\eta = 2.31 \%$) of the CB cell device. This result suggests that the film morphology slightly improved compared to that using CB solvent because the solvent evaporation rate changed. We also investigated the performance change of the DCT:CHL devices by applying a drying treatment to the as-prepared PCBM:P3HT blend films. Figure 7 shows the surface AFM images of PCBM:P3HT blend films which was heated from $25 \text{ }^\circ\text{C}$ to $200 \text{ }^\circ\text{C}$ for 20 min on a hot plate. The height differences in the PCBM:P3HT films drying above $90 \text{ }^\circ\text{C}$ were below 20 nm although those in the films drying below $60 \text{ }^\circ\text{C}$ were ca. 45 nm. Figure 8 shows the plots of the Root Mean Square Roughness (RMS) for those PCBM:P3HT blend films estimated by the AFM measurement and the η of the cosolvent cell device against the drying temperature. When the blend films were dried at $20 \text{ }^\circ\text{C}$ and $60 \text{ }^\circ\text{C}$, the RMS values were large and the η values were about 1.7 % ~ 2.0 %. Whereas, when the blend films were dried at $90 \text{ }^\circ\text{C}$ and $120 \text{ }^\circ\text{C}$, the RMS values were small and the η increased up to 2.3 % ~ 2.5 %. These results imply that both of PCBM and P3HT domains in the blend film were distributed finely by drying at about $100 \text{ }^\circ\text{C}$, leading to an increase in charge separation interface. However when the blend films were dried at $150 \text{ }^\circ\text{C}$ and $200 \text{ }^\circ\text{C}$, the RMS values

were smaller than those dried below 120 °C but the η decreased. Glass transition point of P3HT is about 100 °C ~ 130 °C although the properties such as molecular weight of P3HT influence the point. The blend film can have more flat surface by heating above the glass transition point, but the phase separation between PCBM and P3HT domains may proceed resulting in lower device performance because of the decrease in the photo-charge separation interfaces.

The inverted type organic solar cells with amorphous TiO_x showed the high durability for 20 h in air as seen in Figure 5. However, when the cell was continuously irradiated for 120 h in air, the η decreased down to 29.3 % of the maximum value as seen by the plot of the open square in Figure 9. Although this reason is incompletely understood at present, charge transfer complexes formed between oxygen and P3HT or singlet oxygen formed by energy-transfer from excited state P3HT may cause cleavages of P3HT polymer chains. In order to suppress this decrease of the cell performance, the device was sealed using a glass plate with water getter sheet. Although the durability was partly improved by sealing the normal type solar cell, the η decreased down to 41.8 % of the maximum value after light irradiation for 30 h as seen by the plot of the filled circle in Figure 9. The performance degradation of this device with sealing may be ascribed to the oxidation of the Al electrode caused by slightly residual oxygen and moisture, despite the device was sealed in the N_2 filled glove box containing trace O_2 and H_2O of less than 1 ppm. Whereas, the amorphous TiO_x inserted type organic solar cells with sealing maintained 96.3 % of the maximum $\eta = 2.45$ % value even after continuous light irradiation for 120 h as seen by the plot of the filled square in Figure 9. This durability improvement is due to preventing a photo-degradation of the PCBM:P3HT blend being promoted by the permeation of oxygen and moisture. Thus, highly durable organic solar cell was obtained by the combination of the relatively air-stable device and the sealing treatment.

We believe that the stability of our cell is extremely high, although we cannot compare easily the durability of organic solar cells since its evaluation method is not standardized.

4. Conclusions

The present paper reported the development and the performance evaluation of the inverted type organic solar cells inserting an amorphous TiO_x layer between the ITO substrate and the P3HT:PCBM blend layer. The η of 2.47 % was observed for the inverted type organic solar cell with the amorphous TiO_x layer showing the high durability even after continuous irradiation of AM 1.5G-100 mW cm^{-2} simulated sunlight for 20 h. This implies that the amorphous TiO_x plays an important role as the electron collection layer and the hole blocking layer and further for the air-stability. In addition, when this device was sealed with a glass plate, it became much air-stable and maintained the relative efficiency over 96 % under continuous irradiation for 120 h. In this way, long lifetime of organic solar cells is expected by employing non-corrosive and air-stable electrode materials, but we have not completely understood yet why their devices are stable and what factors lead to lower their durability. We are under investigating extensively on organic solar cells using n-type semiconductors to develop high performance and long lifetime device.

Acknowledgements

This work was supported by the Incorporated Administrative Agency New Energy and Industrial Technology Development Organization (NEDO) under Ministry of Economy, Trade and Industry (METI).

References

- [1] C. W. Tang, Two-layer organic photovoltaic cell, *Appl. Phys. Lett.* 48 (1986) 183 - 185.
- [2] N. S. Sariciftci, L. Smilowitz, A. J. Heeger, F. Wudl, Photoinduced Electron Transfer from a Conducting Polymer to Buckminsterfullerene, *Science* 258 (1992) 1474 - 1476.
- [3] G. Yu, J. Gao, J. C. Hummelen, F. Wudl, A. J. Heeger, Polymer Photovoltaic Cells: Enhanced Efficiencies via a Network of Internal Donor-Acceptor Heterojunctions, *Science* 270 (1995) 1789 - 1791.
- [4] K. M. Coakley, M. D. McGehee, Conjugated Polymer Photovoltaic Cells, *Chem. Mater.* 16 (2004) 4533 - 4542.
- [5] H. Spanggaard, F. C. Krebs, A brief history of the development of organic and polymeric photovoltaics, *Sol. Energy Mater. Sol. Cells* 83 (2004) 125 - 146.
- [6] S. Gunes, H. Neugebauer, N. S. Sariciftci, Conjugated Polymer-Based Organic Solar Cells, *Chem. Rev.* 107 (2007) 1324 - 1338.
- [7] J. Y. Kim, S. H. Kim, H.-H. Lee, K. Lee, W. Ma, X. Gong, A. J. Heeger, New Architecture for High-Efficiency Polymer Photovoltaic Cells Using Solution-Based Titanium Oxide as an Optical Spacer, *Adv. Mater.* 18 (2006) 572 - 576.
- [8] J. Y. Kim, K. Lee, N. E. Coates, D. Moses, T.-Q. Nguyen, M. Dante, A. J. Heeger, Efficient Tandem Polymer Solar Cells Fabricated by All-Solution Processing, *Science* 317 (2007) 222 - 225.
- [9] M. D. Irwin, D. B. Buchholz, A. W. Hains, R. P. H. Chang, T. J. Marks, p-Type semiconducting nickel oxide as an efficiency-enhancing anode interfacial layer in polymer bulk-heterojunction solar cells, *Proc. Natl. Acad. Sci. USA* 105 (2008) 2783 - 2787.
- [10] C. J. Brabec, N. S. Sariciftci, J. C. Hummelen, Plastic Solar Cells, *Adv. Funct. Mater.* 11 (2001) 15 - 26.

- [11] J. A. Hauch, P. Schilinsky, S. A. Choulis, R. Childers, M. Biele, C. J. Brabec, Flexible organic P3HT:PCBM bulk-heterojunction modules with more than 1 year outdoor lifetime, *Sol. Energy Mater. Sol. Cells* 92 (2008) 727 - 731.
- [12] F. C. Krebs, H. Spanggaard, Significant Improvement of Polymer Solar Cell Stability, *Chem. Mater.* 17 (2005) 5235 - 5237.
- [13] M. Jorgensen, K. Norrman, F. C. Krebs, Stability/degradation of polymer solar cells, *Sol. Energy Mater. Sol. Cells* 92 (2008) 686 - 714.
- [14] K. Lee, J. Y. Kim, S. H. Park, S. H. Kim, S. Cho, A. J. Heeger, Air-Stable Polymer Electronic Devices, *Adv. Mater.* 19 (2007) 2445 - 2449.
- [15] F. C. Krebs, Air stable polymer photovoltaics based on a process free from vacuum steps and fullerenes, *Sol. Energy Mater. Sol. Cells* 92 (2008) 715 - 726.
- [16] K. Takahashi, I. Nakajima, K. Imoto, T. Yamaguchi, T. Komura, K. Murata, Sensitization effect by porphyrin in polythiophene/perylene dye two-layer solar cells, *Sol. Energy Mater. Sol. Cells* 76 (2003) 115 - 124.
- [17] J.-i. Nakamura, S. Suzuki, K. Takahashi, C. Yokoe, K. Murata, The Photovoltaic Mechanism of a Polythiophene/Perylene Pigment Two-Layer Solar Cell, *Bull. Chem. Soc. Jpn.* 77 (2004) 2185 - 2188.
- [18] K. Takahashi, K. Seto, T. Yamaguchi, J.-i. Nakamura, C. Yokoe, K. Murata, Performance Enhancement by Blending an Electron Acceptor in TiO_2 /polyphenylenevinylene/Au Solid-state Solar Cells, *Chem. Lett.* 33 (2004) 1042 - 1043.
- [19] K. Takahashi, Y. Takano, T. Yamaguchi, J.-i. Nakamura, C. Yokoe, K. Murata, Porphyrin dye-sensitization of polythiophene in a conjugated polymer/ TiO_2 p-n hetero-junction solar cell, *Synth. Met.* 155 (2005) 51 - 55.

- [20] J.-i. Nakamura, C. Yokoe, K. Murata, K. Takahashi, Efficient organic solar cells by penetration of conjugated polymers into perylene pigments, *J. Appl. Phys.* 96 (2004) 6878 - 6883.
- [21] C. Waldauf, M. Morana, P. Denk, P. Schilinsky, K. Coakley, S. A. Choulis, C. J. Brabec, Highly efficient inverted organic photovoltaics using solution based titanium oxide as electron selective contact, *Appl. Phys. Lett.* 89 (2006) 233517-1 - 3.
- [22] R. Steim, S. A. Choulis, P. Schilinsky, C. J. Brabec, Interface modification for highly efficient organic photovoltaics, *Appl. Phys. Lett.* 92 (2008) 093303-1 - 3.
- [23] A. Hayakawa, O. Yoshikawa, T. Fujieda, K. Uehara, S. Yoshikawa, High performance polythiophene/fullerene bulk-heterojunction solar cell with a TiO_x hole blocking layer, *Appl. Phys. Lett.* 90 (2007) 163517-1 - 3.
- [24] M. Takahashi, K. Tsukigi, T. Uchino, T. Yoko, Enhanced photocurrent in thin film TiO₂ electrodes prepared by sol-gel method, *Thin Solid Films* 388 (2001) 231 - 236.
- [25] K. Pomoni, A. Vomvas, C. Trapalis, Transient photoconductivity of nanocrystalline TiO₂ sol-gel thin films, *Thin Solid Films* 479 (2005) 160 - 165.

Table 1 Device performance of the inverted type solar cells* with various TiO_x layers under light irradiation of the simulated sunlight AM1.5G-100 mW cm⁻².

	$J_{sc} / \text{mA cm}^{-2}$	V_{oc} / V	FF	$\eta / \%$	R_s / Ω	R_p / Ω
EA-TiO _x	6.70	0.56	0.55	2.06	17.4	699.3
DEA-TiO _x	5.31	0.55	0.36	1.06	49.9	272.5
AA-TiO _x	7.00	0.55	0.60	2.31	14.2	813.0

* The PCBM:P3HT blend film was prepared using the CB.

Table 2 Durability of the inverted type solar cell* with amorphous AA-TiO_x layer and the normal type solar cell* with Al electrode under continuous irradiation in air of the simulated sunlight AM1.5G-100 mW cm⁻².

Irradiation time / h	Energy conversion yield of inverted type cell / %	Energy conversion yield of normal type cell / %
0	2.20	2.11
5	2.21	1.28
10	2.19	1.04
20	2.13	-
RE	95.8%	49.3 %

RE; relative efficiency.

The RE was calculated by $RE = \eta_{con} / \eta_{max}$, where the η_{con} and the η_{max} are the η value when the continuous irradiation measurement was stopped and the maximum η value, respectively.

* The PCBM:P3HT blend film was prepared using the CB.

Figure captions

Figure 1 Schematic structures of normal (a) and inverted type organic solar cells (b), and a cross-sectional SEM image of the ITO/TiO_x/PCBM:P3HT/PEDOT:PSS/Au inverted type organic solar cell (c).

Figure 2 I-V curves of inverted type solar cells with (a) and without an amorphous EA-TiO_x layer (b) under light irradiation of AM 1.5G-100 mW cm⁻². Curves (c) and (d) show I-V curves of the cells with and without the TiO_x layer in the dark, respectively. The PCBM:P3HT blend film was prepared using the CB.

Figure 3 I-V curves of inverted type solar cells with various amorphous TiO_x layers prepared from EA-TiO_x (solid line (a)), DEA-TiO_x (dash line (b)), and AA-TiO_x (dot line (c)) under light irradiation of AM 1.5G-100 mW cm⁻². The PCBM:P3HT blend film was prepared using the CB. Inset illustrates plots of power conversion efficiency (η) of ITO/TiO_x/PCBM:P3HT/PEDOT:PSS/Au solar cells vs. the thickness of TiO_x layer prepared from EA-TiO_x (open square), DEA-TiO_x (open circle), and AA-TiO_x (open triangle).

Figure 4 Irradiation time dependence of the η for the ITO/AA-TiO_x/PCBM:P3HT/PEDOT:PSS/Au inverted type solar cell under light irradiation of AM 1.5G-100 mW cm⁻² with (open circle) and without UV cut filter (filled circle). The cell was exposed in air during the irradiation. The PCBM:P3HT blend film was prepared using the CB.

Figure 5 Irradiation time dependence of the η for the ITO/AA-TiO_x/PCBM:P3HT/PEDOT:PSS/Au inverted type solar cells with an amorphous

TiO_x layer (open square) and for the ITO/PEDOT:PSS/P3HT:PCBM/Al normal type solar cell (open circle). The cells were exposed in air during the irradiation. The PCBM:P3HT blend film was prepared using the CB.

Figure 6 I-V curves of inverted type solar cells with PCBM:P3HT blend film prepared by chlorobenzene (a) and 2,6-dichlorotoluene:chloroform (DCT:CHL) (b) under light irradiation of AM 1.5G-100 mW cm⁻². AA-TiO_x was used as an electron collector layer.

Figure 7 Drying temperature dependency of the surface AFM images of the PCBM:P3HT blend film prepared by DCT:CHL. Drying temperature; 25 °C (a), 60 °C (b), 90 °C (c), 120 °C (d), 150 °C (e), 200 °C (f). AA-TiO_x was used as an electron collector layer.

Figure 8 Plots of the root mean square roughness (RMS, filled circle) for PCBM:P3HT blend film prepared by DCT:CHL and the η (open circle) of the cosolvent cell device against the drying temperature. AA-TiO_x was used as an electron collector layer.

Figure 9 Comparison of the power conversion efficiency on continuous irradiation time for the ITO/AA-TiO_x/PCBM:P3HT/PEDOT:PSS/Au inverted type organic solar cells with (filled square) and without sealing (open square), and the normal type solar cell with sealing (filled circle). The PCBM:P3HT blend film was prepared using the DCT:CHL.

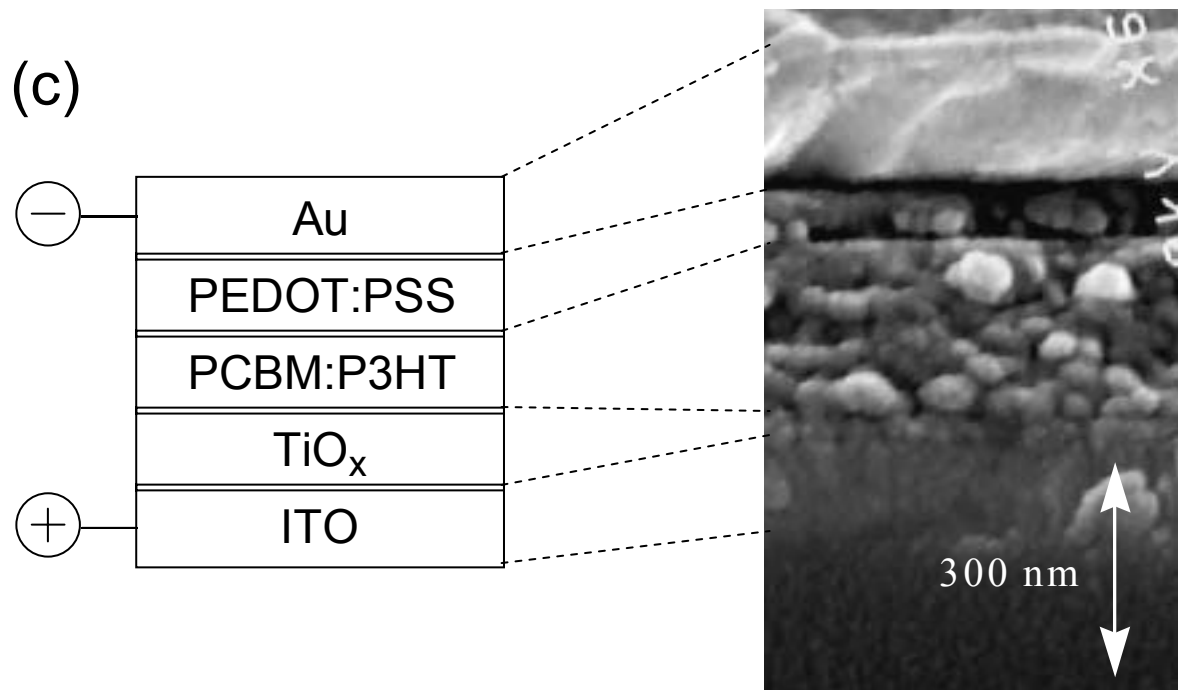
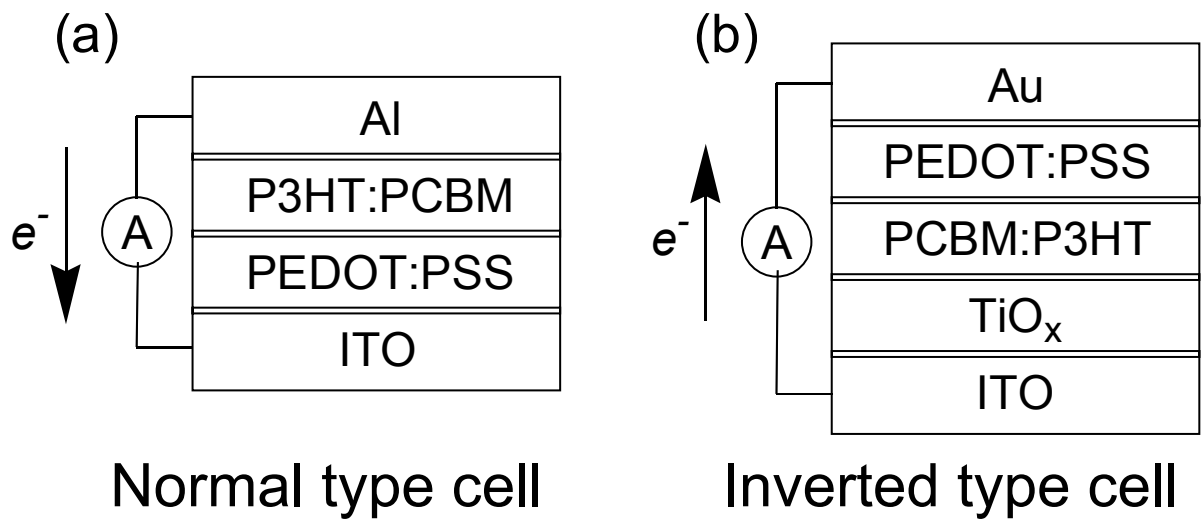


Figure 1

Kuwabara et al.

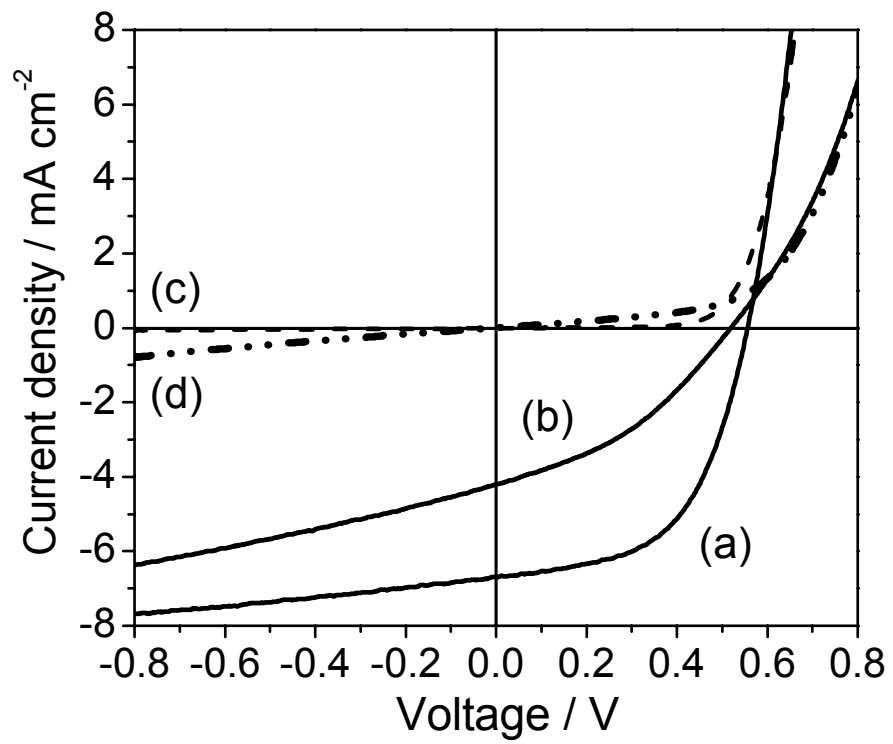


Figure 2

Kuwabara et al.

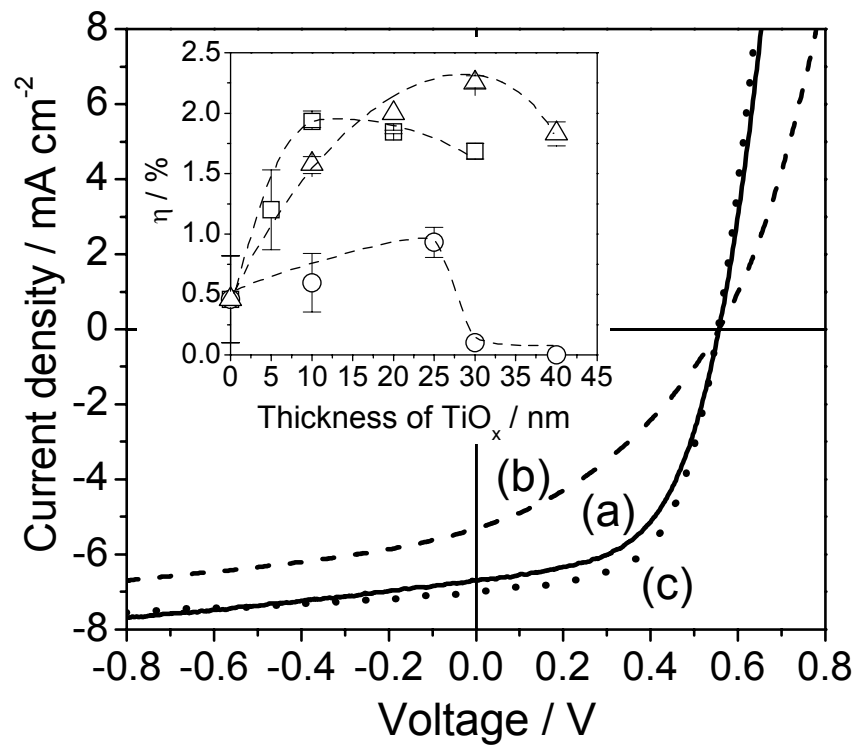


Figure 3

Kuwabara et al.

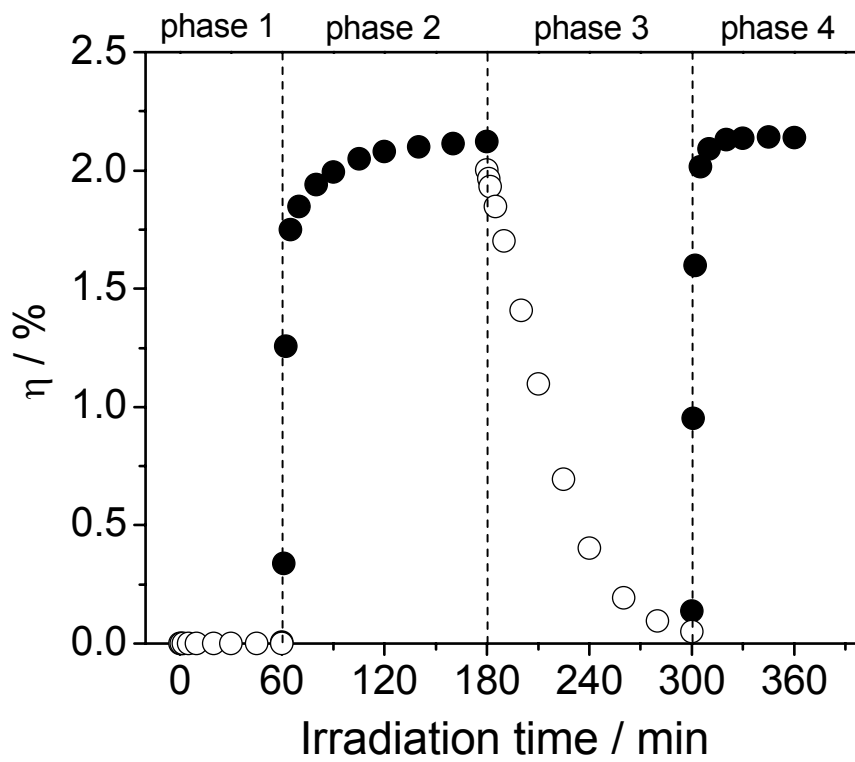


Figure 4

Kuwabara et al.

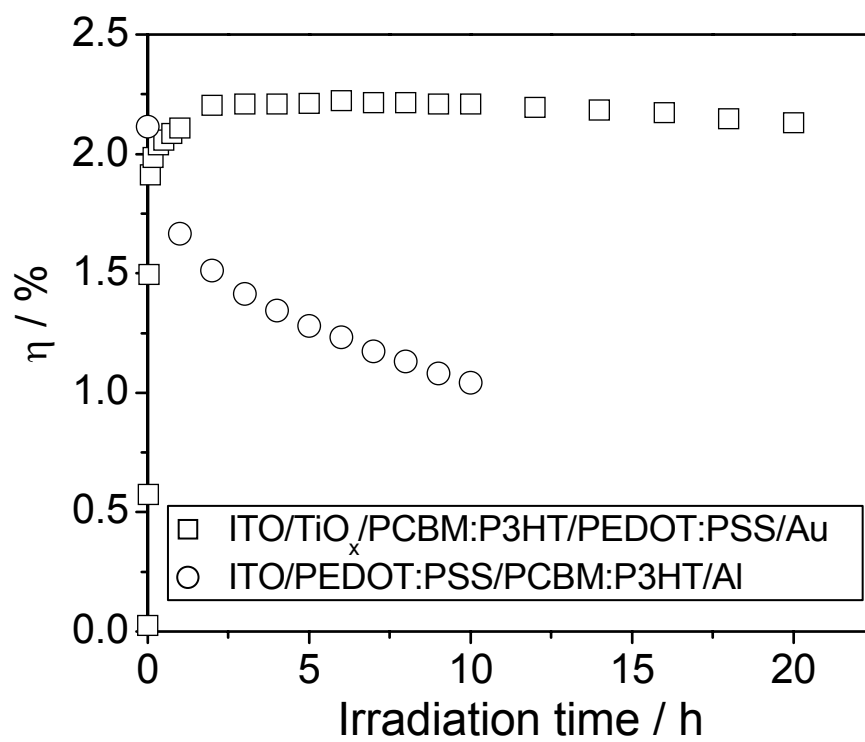


Figure 5

Kuwabara et al.

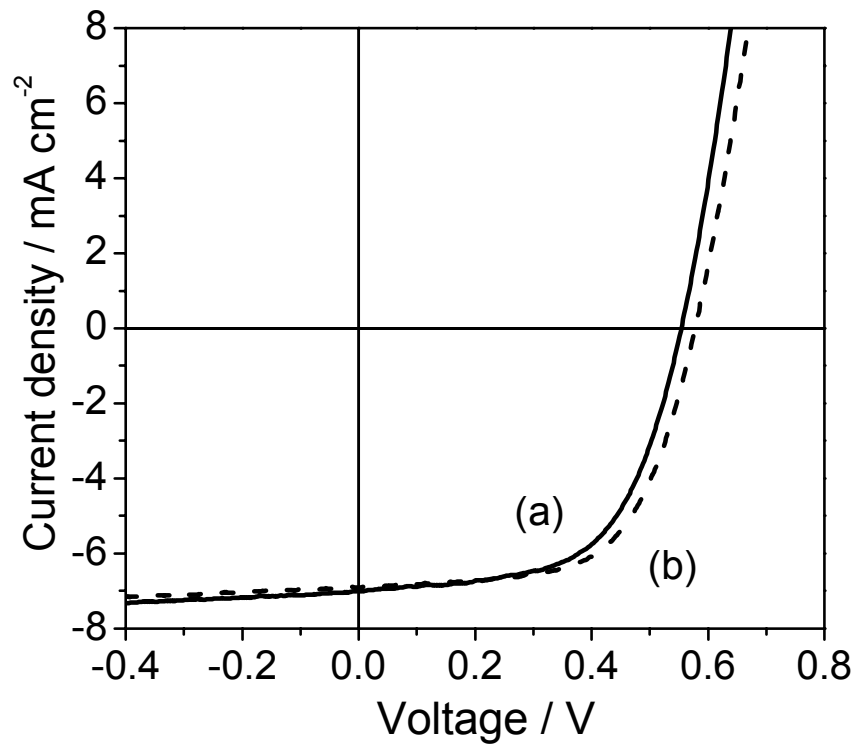


Figure 6

Kuwabara et al.

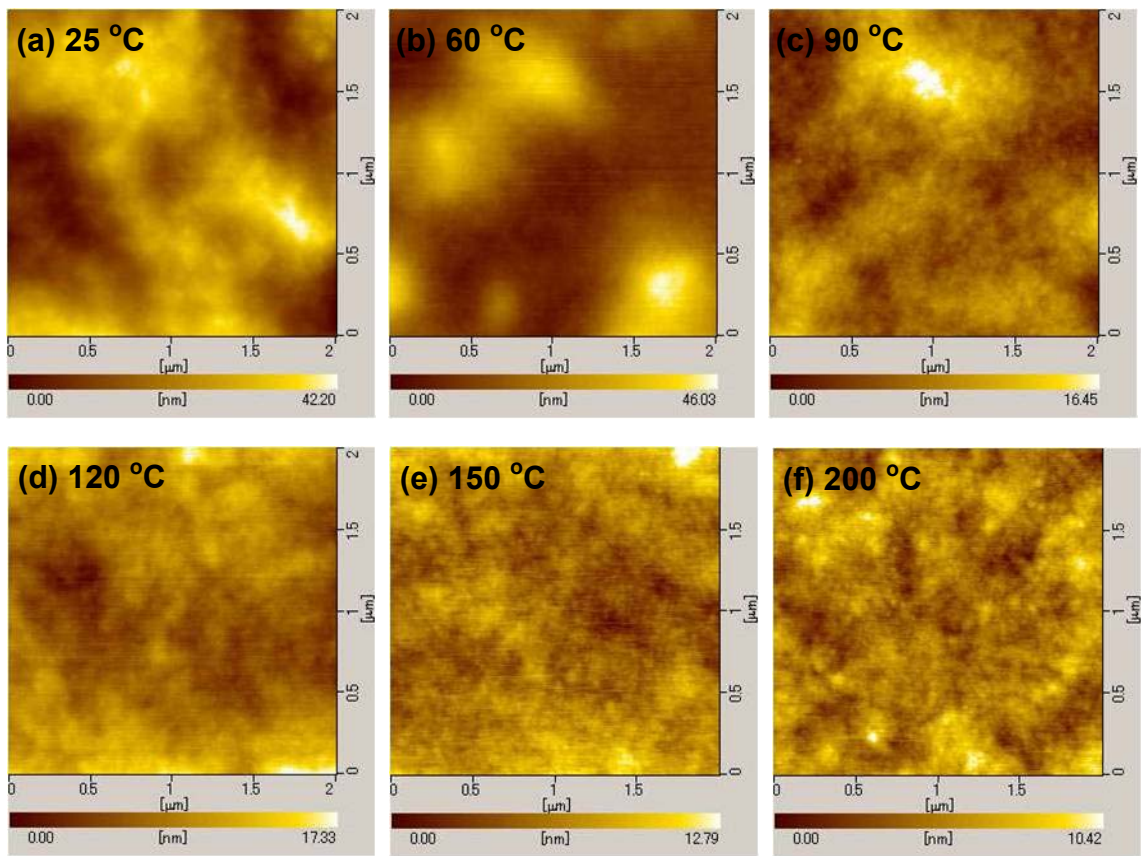


Figure 7

Kuwabara et al.

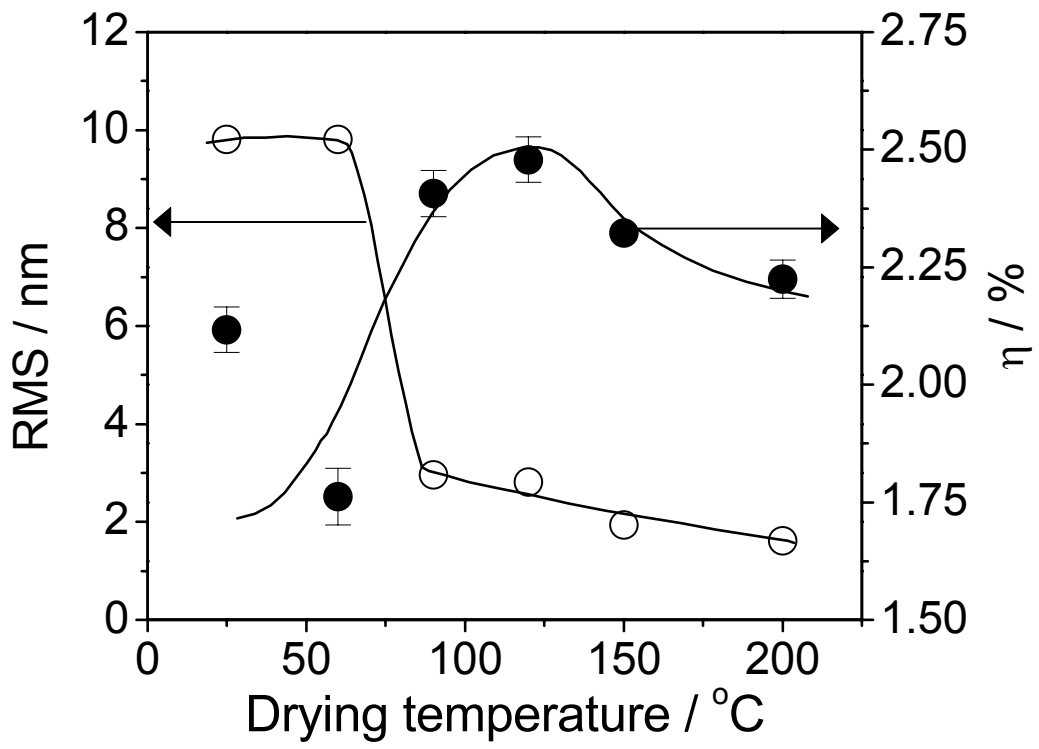


Figure 8

Kuwabara et al.

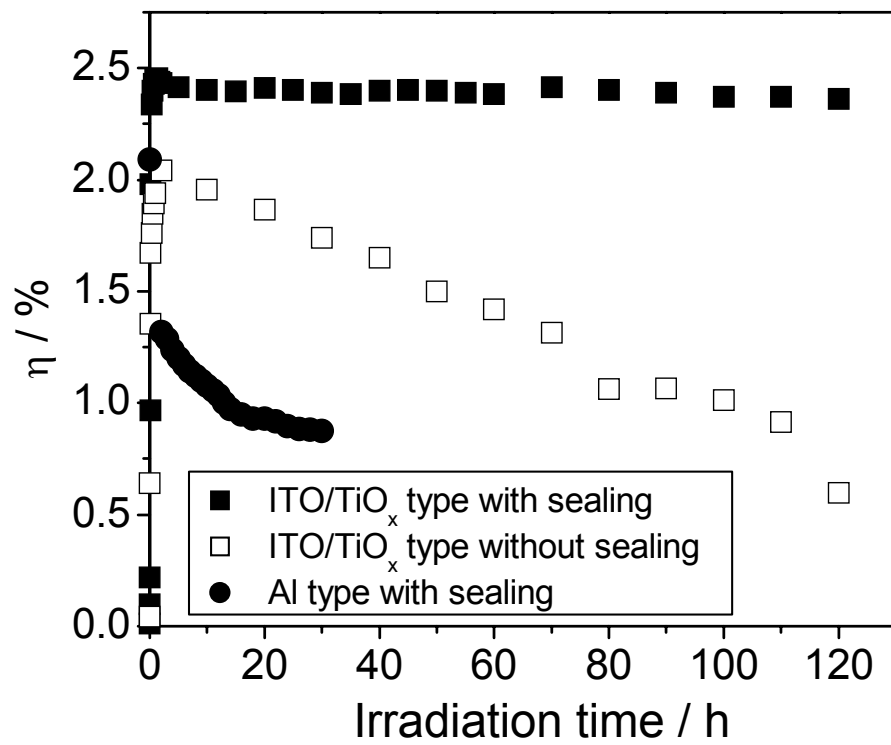


Figure 9

Kuwabara et al.